

IMPORTANCE OF ARRAY REDUNDANCY PATTERN IN ACTIVE SENSING

Robin Rajamäki, Piya Pal

Department of Electrical and Computer Engineering, University of California San Diego, USA

ABSTRACT

This paper further investigates the role of the array geometry and redundancy in active sensing. We are interested in the fundamental question of how many point scatterers can be identified (in the angular domain) by a given array geometry using a certain number of linearly independent transmit waveforms. We consider redundant array configurations (with repeated virtual transmit-receive sensors), which we have recently shown to be able to achieve their maximal identifiability while transmitting fewer independent waveforms than transmitters. Reducing waveform rank in this manner can be beneficial in various ways. For example, it may free up spatial resources for transmit beamforming. In this paper, we show that two array geometries with identical sum co-arrays, and the same number of physical and virtual sensors, need not achieve equal identifiability—regardless of the choice of waveform of a fixed reduced rank. This surprising result establishes the important role the *pattern* (not just the number) of repeated virtual sensors has in governing identifiability, and reveals the limits of compensating for unfavorable array geometries via waveform design.

Index Terms— Sparse arrays, redundancy, active sensing, MIMO radar, waveform design, identifiability

1. INTRODUCTION

Active sensing and sparse arrays play a key role in numerous applications including autonomous sensing [1], automotive radar [2], and emerging wireless systems for joint communications and sensing (JCS) [3,4]. The performance of such systems critically depends on the transmitted waveforms [5–7] as well as the employed transmit (Tx) and receive (Rx) array geometries [8–13]. In particular, multiple-input multiple-output (MIMO) systems can adjust the number of linearly independent waveforms or so-called *waveform rank* (WR) to, e.g., trade off between Tx beamforming gain and field-of-view. In colocated MIMO radar [14], full WR in the form of orthogonal waveforms is conventionally employed to maximize the number of identifiable scatterers. However, since

identifiability is upper bounded by the size of the *sum co-array* [15]—consisting of the pairwise sums of the Tx-Rx sensor positions—a *redundant* array, which has repeated virtual sensors, may actually achieve its maximal identifiability using a reduced WR [16]. This enables redirecting spatial resources towards beamforming or, communications in the case of dual-function JCS systems. Additional advantages of redundant arrays include robustness to sensor failure [17] and resilience to noise due to spatial averaging over repeated virtual sensors.

Until recently, relatively little was known about the impact of array redundancy and WR on identifiability. In our recent work, we showed that maximizing identifiability at a reduced WR requires the Tx waveform to be matched to the array geometry [16]. Indeed, even two waveforms giving rise to *identical* Tx beampatterns can yield different identifiability when employed by the same array. Hence, constraining the Tx beampattern without considering the joint Tx-Rx array geometry may result in suboptimal sensing performance. This perspective gives rise to yet unaddressed questions such as: Is proper waveform design *sufficient* for maximizing identifiability? Can all array geometries of a given size and with identical sum co-arrays achieve the same identifiability simply by choosing the waveforms (of fixed WR) suitably?

This paper answers these questions in the negative. Specifically, we demonstrate that two redundant array geometries can have the same number of physical sensors and identical uniform sum co-arrays, yet different identifiability properties. Surprisingly, *no* choice of waveforms can improve identifiability when employing an unfavorable redundant array geometry and a reduced WR. This novel insight reveals the impact that the configuration of redundant virtual sensors has on identifiability, and highlights the importance of judicious sparse array design, which is especially important in future resource-efficient active sensing systems, such as autonomous sensing and JCS.

2. SIGNAL MODEL

Let the support of unknown K -sparse vector $\mathbf{x} \in \mathbb{C}^V$ encode the angular directions of K far field scatterers, which lie on a grid of $V \gg K$ candidate angles. For a single range-Doppler cell, the Rx vector of a colocated active sensing MIMO sys-

This work was supported in part by grants ONR N00014-19-1-2256, ONR N00014-19-1-2227, NSF 2124929 and DE-SC0022165, as well as the Ulla Tuominen foundation and the Finnish Defence Research Agency.

tem in absence of noise can be modeled as [16, 18, 19]

$$\mathbf{y} = (\mathbf{S} \otimes \mathbf{I})(\mathbf{A}_t \odot \mathbf{A}_r)\mathbf{x} = (\mathbf{S} \otimes \mathbf{I})\mathbf{\Upsilon}\mathbf{A}\mathbf{x} \triangleq \mathbf{B}\mathbf{x}. \quad (1)$$

Here, \otimes and \odot denote the Kronecker and Khatri-Rao (column-wise Kronecker) products, respectively, and \mathbf{I} is the $N_r \times N_r$ identity matrix, where N_r is the number of Rx sensors. Moreover, $\mathbf{S} \in \mathbb{C}^{T \times N_t}$ is a known deterministic *spatio-temporal waveform matrix* (or space-time code [20]) whose columns represent signals of length T launched by the N_t Tx sensors. The effective Tx-Rx manifold matrix $\mathbf{A}_t \odot \mathbf{A}_r \in \mathbb{C}^{N_t N_r \times V}$ models the phase shifts incurred by the narrowband radiation transmitted/received by the arrays. Since $\mathbf{A}_t \odot \mathbf{A}_r$ can have repeated rows, we may write $\mathbf{A}_t \odot \mathbf{A}_r = \mathbf{\Upsilon}\mathbf{A}$, where $\mathbf{A} \in \mathbb{C}^{N_\Sigma \times V}$ is the manifold matrix of a virtual array (independent of \mathbf{S}) with $N_\Sigma \leq N_t N_r$ unique virtual sensors. This so-called *sum co-array* [21], denoted by \mathbb{D}_Σ , is defined as

$$\mathbb{D}_\Sigma \triangleq \mathbb{D}_t + \mathbb{D}_r = \{d_t + d_r \mid d_t \in \mathbb{D}_t; d_r \in \mathbb{D}_r\}, \quad (2)$$

where $\mathbb{D}_t \triangleq \{d_t[n]\}_{n=1}^{N_t}$ and $\mathbb{D}_r \triangleq \{d_r[m]\}_{m=1}^{N_r}$ are the set of Tx and Rx sensor positions, respectively. Furthermore, $\mathbf{\Upsilon} \in \{0, 1\}^{N_t N_r \times N_\Sigma}$ is the so-called *redundancy pattern* matrix mapping the $N_\Sigma \triangleq |\mathbb{D}_\Sigma|$ unique virtual sensors in \mathbb{D}_Σ ($|\mathbb{D}_\Sigma|$ denotes the cardinality of \mathbb{D}_Σ) to the corresponding physical Tx-Rx sensor pairs (d_t, d_r) .

Definition 1 (Redundancy pattern). *The (n, ℓ) th entry of the binary redundancy pattern matrix $\mathbf{\Upsilon} \in \{0, 1\}^{N_t N_r \times N_\Sigma}$ is*

$$\Upsilon_{n,\ell} \triangleq \begin{cases} 1, & \text{if } d_t[\lceil \frac{n}{N_r} \rceil] + d_r[n - (\lceil \frac{n}{N_r} \rceil - 1)N_r] = d_\Sigma[\ell] \\ 0, & \text{otherwise.} \end{cases}$$

Here, $d_\Sigma[\ell] \in \mathbb{D}_\Sigma$ is the ℓ th sum co-array element position, and $\lceil \cdot \rceil$ denotes the ceiling function.

An array is *redundant* if $N_\Sigma < N_t N_r$ and nonredundant if $N_\Sigma = N_t N_r$. Furthermore, sum co-array \mathbb{D}_Σ is *contiguous* if $\mathbb{D}_\Sigma = \{0, 1, \dots, N_\Sigma - 1\}$, where $\mathbb{D}_t, \mathbb{D}_r \supseteq \{0\}$ are assumed to be non-negative integer sets describing the normalized Tx/Rx sensor positions in units of half the carrier wavelength. For a contiguous sum co-array, the (ℓ, i) th entry of \mathbf{A} is thus $A_{\ell,i} = \exp(j\pi(\ell - 1) \sin \theta_i)$, where $\theta_i \in [-\frac{\pi}{2}, \frac{\pi}{2})$.

We are interested in understanding the interplay between the spatial sensing geometry (captured by $\mathbf{\Upsilon}\mathbf{A}$) and the waveform \mathbf{S} that maximizes the number of identifiable scatterers (i.e., the size of the support of \mathbf{x}). It is well-known that the sparsest solution to $\mathbf{y} = \mathbf{B}\mathbf{x}$ is unique if and only if $K \leq \frac{1}{2} \text{k-rank}(\mathbf{B})$ [22, 23], where $\text{k-rank}(\mathbf{B})$ denotes the Kruskal rank¹ of matrix \mathbf{B} . Due to the spatio-temporal structure of \mathbf{B} , its Kruskal rank is determined by the (i) sum co-array, which is modeled by virtual manifold matrix \mathbf{A} , (ii)

redundancy pattern $\mathbf{\Upsilon}$, and (iii) waveform matrix \mathbf{S} . A key quantity of interest is the waveform rank (WR), defined as

$$N_s \triangleq \text{rank}(\mathbf{S}). \quad (3)$$

The case $N_s = 1$ corresponds to the phased array, whereas a canonical example of $N_s = N_t$ is (orthogonal) MIMO radar, which is known to achieve maximal Kruskal rank $\text{k-rank}(\mathbf{B}) = N_\Sigma$ [15, 16]. Advantages of a reduced waveform rank $N_s < N_t$ include improved beamforming gain on transmit, fewer costly RF chains at the transmitter, and possibly decreased transmission time, since $T \geq N_s$. It is therefore important to understand (a) if maximal Kruskal rank can be attained for a given array at a reduced N_s , and (b) which choices of \mathbf{S} enable this. To answer these questions, we briefly review the key ideas of *array-informed waveform design* introduced in [16].

3. ARRAY-INFORMED WAVEFORM DESIGN IN A NUTSHELL

Fig. 1 illustrates the range of values that the Kruskal rank of \mathbf{B} may assume as a function of the WR given an arbitrary array with N_t Tx sensors, N_r Rx sensors, and N_Σ virtual sensors [16].² The design space (shaded area) is upper bounded by the *maximal* Kruskal rank [16]

$$\text{k-rank}(\mathbf{B}) \leq \min(N_s N_r, N_\Sigma), \quad (4)$$

which is a piecewise linear function in N_s tracing the set of identifiability-maximizing operating points. Eq. (4) reveals the existence of an *optimal* operating point $N_s = \lceil N_\Sigma / N_r \rceil$, which is the minimum WR needed to attain maximal Kruskal rank N_Σ . A key observation is that setting $N_s > \lceil N_\Sigma / N_r \rceil$ can be wasteful for redundant arrays, since $N_t - \lceil N_\Sigma / N_r \rceil$ Tx degrees of freedom could instead be used to, e.g., beamform, or serve users in dual-function JCS systems, without sacrificing identifiability.

The upper bound in (4) can be attained for any N_t, N_r, N_s and suitable values of N_Σ [16]. This requires both proper array design and “matching” waveform matrix \mathbf{S} to the array geometry or redundancy pattern $\mathbf{\Upsilon}$. We call this “array-informed waveform design”. Intuitively, an \mathbf{S} that maximizes identifiability should minimize the dimension of the intersection between the null space of $\mathbf{S} \otimes \mathbf{I}$ and range space of $\mathbf{\Upsilon}$. In the redundancy-limited regime $N_s \geq N_\Sigma / N_r$, where Kruskal rank N_Σ could potentially be attained, the following necessary and sufficient condition for $\text{k-rank}(\mathbf{B}) = N_\Sigma$ holds.

Proposition 1 (Redundancy-limited waveform rank [16, Theorem 2]). *If $\text{rank}(\mathbf{S}) \geq N_\Sigma / N_r$, then*

$$\text{k-rank}(\mathbf{B}) = N_\Sigma \iff \begin{cases} \text{k-rank}(\mathbf{A}) = N_\Sigma \text{ and} \\ \text{rank}((\mathbf{S} \otimes \mathbf{I})\mathbf{\Upsilon}) = N_\Sigma. \end{cases} \quad (5)$$

¹The Kruskal rank of matrix \mathbf{B} , denoted $\text{k-rank}(\mathbf{B})$, is the largest integer r such that every r columns of \mathbf{B} are linearly independent.

²There can be multiple arrays with the same N_Σ but different redundancy patterns $\mathbf{\Upsilon}$ for a given N_t, N_r .

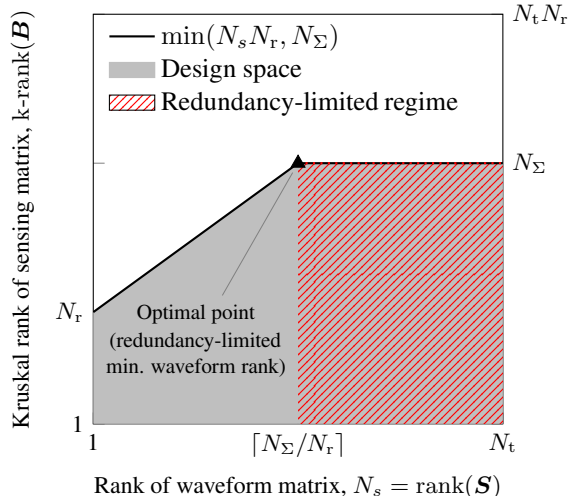


Fig. 1. Array-dependent trade-off between N_s and $\text{k-rank}(\mathbf{B})$. The set of optimal operating points—in terms of identifiability—are given by the maximal Kruskal rank in (4). Optimal point ($\lceil \frac{N_\Sigma}{N_r} \rceil, N_\Sigma$) represents the minimum waveform rank achieving the maximum (redundancy-limited) Kruskal rank. Here, N_t , N_r and N_Σ denote the number of Tx, Rx, and virtual sensors, respectively.

The utility of Proposition 1 stems from the fact that if the sum co-array is contiguous, then \mathbf{A} is a Vandermonde matrix and $\text{k-rank}(\mathbf{A}) = N_\Sigma$. Hence, verifying the computationally challenging Kruskal rank condition $\text{k-rank}(\mathbf{B}) = N_\Sigma$ reduces to the simpler condition $\text{rank}((\mathbf{S} \otimes \mathbf{I})\mathbf{Y}) = N_\Sigma$.

This paper delves deeper into the question “what combination of array geometry and waveform can achieve maximal Kruskal rank in the redundancy-limited regime?” When $N_s = N_t$, it can easily be verified that any array with a contiguous sum co-array achieves $\text{k-rank}(\mathbf{B}) = N_\Sigma$, regardless of the choice of \mathbf{S} (of rank N_t) [16]. However, the answer is not so obvious when $N_s < N_t$. The optimal point $N_s = \lceil N_\Sigma / N_r \rceil$ in Fig. 1 is of particular interest. Hence, the remainder of the paper focuses on *whether Kruskal rank N_Σ is always attainable with minimum WR*. Specifically, given any array geometry with a contiguous co-array of a fixed size N_Σ , does there always exist a choice of \mathbf{S} such that $\text{k-rank}(\mathbf{B}) = N_\Sigma$ when $N_s = \lceil N_\Sigma / N_r \rceil$? Interestingly, the answer is *no*, as we show next.

4. IMPORTANCE OF REDUNDANCY PATTERN FOR MAXIMIZING IDENTIFIABILITY

This section demonstrates that the maximum *achievable* Kruskal rank of a given array geometry depends on redundancy pattern \mathbf{Y} ; *not* solely on tuple $(N_t, N_r, N_\Sigma, N_s)$. Hence, the solid black line in Fig. 1 may be attained for all N_s by one array geometry, but not another with the same contiguous co-array, and number of physical/virtual sensors

N_t, N_r, N_Σ —regardless of the choice of waveform matrix \mathbf{S} .

Theorem 1. *There exists two array geometries with contiguous sum co-arrays and the same N_t, N_r, N_Σ such that the associated spatio-temporal sensing matrices \mathbf{B}_I and \mathbf{B}_{II} obey $\text{k-rank}(\mathbf{B}_I) < N_\Sigma$ and $\text{k-rank}(\mathbf{B}_{II}) = N_\Sigma$ when $N_s = \lceil N_\Sigma / N_r \rceil$.*

Remark 1. *Theorem 1 shows the importance of proper array design for maximizing identifiability, as two arrays with the same (contiguous) sum co-array and number of physical/virtual sensors need not achieve equal identifiability. An unfavorable redundancy pattern can thus limit identifiability.*

To show existence in Theorem 1, it suffices to construct two array configurations for specific values of N_t, N_r , and N_Σ . This conveys the essential idea of the proof technique. A more general proof, including extensions to other values of $(N_t, N_r, N_\Sigma, N_s)$, is part of ongoing work.

4.1. Proof sketch of Theorem 1

Consider the following two array geometries:

- I. $\mathbb{D}_t = \{0, 1, 2\}$ and $\mathbb{D}_r = \{0, 1, 2, 5\}$
- II. $\mathbb{D}_t = \{0, 1, 2\}$ and $\mathbb{D}_r = \{0, 1, 3, 5\}$.

These configurations differ only in the position of a single Rx sensor (highlighted in red), as illustrated in Fig. 2. The corresponding redundancy patterns \mathbf{Y}_I and \mathbf{Y}_{II} are

$$\mathbf{Y}_I = \begin{bmatrix} 1 & 0 & 0 & 0 & 0 & 0 & 0 & 0 \\ 0 & 1 & 0 & 0 & 0 & 0 & 0 & 0 \\ 0 & 0 & \color{red}{1} & 0 & 0 & 0 & 0 & 0 \\ 0 & 0 & 0 & 0 & 0 & 1 & 0 & 0 \\ 0 & 1 & 0 & 0 & 0 & 0 & 0 & 0 \\ 0 & 0 & 1 & 0 & 0 & 0 & 0 & 0 \\ 0 & 0 & 0 & \color{red}{1} & 0 & 0 & 0 & 0 \\ 0 & 0 & 0 & 0 & 0 & 0 & 1 & 0 \\ 0 & 0 & 1 & 0 & 0 & 0 & 0 & 0 \\ 0 & 0 & 0 & 1 & 0 & 0 & 0 & 0 \\ 0 & 0 & 0 & 0 & \color{red}{1} & 0 & 0 & 0 \\ 0 & 0 & 0 & 0 & 0 & 0 & 0 & 1 \end{bmatrix}, \mathbf{Y}_{II} = \begin{bmatrix} 1 & 0 & 0 & 0 & 0 & 0 & 0 & 0 \\ 0 & 1 & 0 & 0 & 0 & 0 & 0 & 0 \\ 0 & 0 & 0 & \color{red}{1} & 0 & 0 & 0 & 0 \\ 0 & 0 & 0 & 0 & 0 & 1 & 0 & 0 \\ 0 & 1 & 0 & 0 & 0 & 0 & 0 & 0 \\ 0 & 0 & 1 & 0 & 0 & 0 & 0 & 0 \\ 0 & 0 & 0 & 0 & \color{red}{1} & 0 & 0 & 0 \\ 0 & 0 & 0 & 0 & 0 & 0 & 1 & 0 \\ 0 & 0 & 1 & 0 & 0 & 0 & 0 & 0 \\ 0 & 0 & 0 & 1 & 0 & 0 & 0 & 0 \\ 0 & 0 & 0 & 0 & \color{red}{1} & 0 & 0 & 0 \\ 0 & 0 & 0 & 0 & 0 & 0 & 0 & 1 \end{bmatrix}.$$

Both arrays have a contiguous sum co-array with $N_\Sigma = 8$ virtual sensors. Nevertheless, Array I *cannot* achieve maximal Kruskal rank for $N_s = N_\Sigma / N_r = 2$, unlike Array II. This is shown next using Proposition 1, which reduces to analyzing the rank of $\mathbf{W}_i \triangleq (\mathbf{S} \otimes \mathbf{I})\mathbf{Y}_i$, $i \in \{I, II\}$, since \mathbf{A} is Vandermonde and has full Kruskal rank both for Arrays I and II.

By assumption, $N_s = 2$. Let also $T = 2$ such that

$$\mathbf{S} = \begin{bmatrix} s_{11} & s_{12} & s_{13} \\ s_{21} & s_{22} & s_{23} \end{bmatrix}. \quad (6)$$

We may consider (6) without loss of generality for the purpose of applying Proposition 1, since for any $\mathbf{S}' \in \mathbb{C}^{T' \times N_t}$

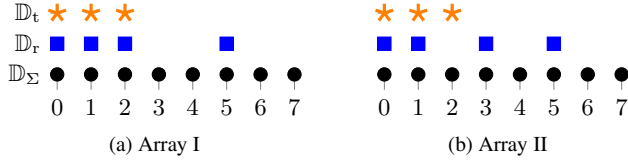


Fig. 2. Array geometries achieving different identifiability despite having an equal number of physical sensors and identical contiguous sum co-arrays. Array II attains the maximal Kruskal rank $N_\Sigma = 8$ when $N_s = N_\Sigma/N_r = 2$, but not Array I.

such that $\text{rank}(\mathbf{S}') = N_s$, any rank-revealing decomposition $\mathbf{S}' = \mathbf{U}\mathbf{S}$, where $\mathbf{U} \in \mathbb{C}^{T' \times N_s}$ and $\mathbf{S} \in \mathbb{C}^{N_s \times N_t}$ have full column and row rank, respectively (the columns of \mathbf{U} span the range space of \mathbf{S}'), implies $\text{rank}((\mathbf{S}' \otimes \mathbf{I})\mathbf{Y}) = \text{rank}((\mathbf{U} \otimes \mathbf{I})(\mathbf{S} \otimes \mathbf{I})\mathbf{Y}) = \text{rank}((\mathbf{S} \otimes \mathbf{I})\mathbf{Y})$.

In case of Array I, \mathbf{W}_I reduces to

$$\mathbf{W}_I = \begin{bmatrix} s_{11} & s_{12} & s_{13} & 0 & 0 & 0 & 0 & 0 \\ 0 & s_{11} & s_{12} & s_{13} & 0 & 0 & 0 & 0 \\ 0 & 0 & s_{11} & s_{12} & s_{13} & 0 & 0 & 0 \\ 0 & 0 & 0 & 0 & 0 & s_{11} & s_{12} & s_{13} \\ s_{21} & s_{22} & s_{23} & 0 & 0 & 0 & 0 & 0 \\ 0 & s_{21} & s_{22} & s_{23} & 0 & 0 & 0 & 0 \\ 0 & 0 & s_{21} & s_{22} & s_{23} & 0 & 0 & 0 \\ 0 & 0 & 0 & 0 & 0 & s_{21} & s_{22} & s_{23} \end{bmatrix}.$$

The last three columns of \mathbf{W}_I are clearly linearly dependent. Hence, \mathbf{W}_I is rank-deficient when $N_s = 2$, i.e., $\text{rank}(\mathbf{W}_I) < N_\Sigma \implies \text{k-rank}(\mathbf{B}_I) < N_\Sigma$, where $\mathbf{B}_I \triangleq \mathbf{W}_I \mathbf{A}$.

In case of Array II, \mathbf{W}_{II} evaluates to

$$\mathbf{W}_{II} = \begin{bmatrix} s_{11} & s_{12} & s_{13} & 0 & 0 & 0 & 0 & 0 \\ 0 & s_{11} & s_{12} & s_{13} & 0 & 0 & 0 & 0 \\ 0 & 0 & 0 & s_{11} & s_{12} & s_{13} & 0 & 0 \\ 0 & 0 & 0 & 0 & 0 & s_{11} & s_{12} & s_{13} \\ s_{21} & s_{22} & s_{23} & 0 & 0 & 0 & 0 & 0 \\ 0 & s_{21} & s_{22} & s_{23} & 0 & 0 & 0 & 0 \\ 0 & 0 & 0 & s_{21} & s_{22} & s_{23} & 0 & 0 \\ 0 & 0 & 0 & 0 & 0 & s_{21} & s_{22} & s_{23} \end{bmatrix}.$$

There exists infinitely many choices of \mathbf{S} yielding a full rank \mathbf{W}_{II} . For example, setting $s_{11}, s_{13}, s_{22} \in \mathbb{C} \setminus \{0\}$ and $s_{12} = s_{21} = s_{23} = 0$ can be verified to ensure that $\text{rank}(\mathbf{S}) = 2$ and $\text{rank}(\mathbf{W}_{II}) = N_\Sigma \implies \text{k-rank}(\mathbf{B}_{II}) = N_\Sigma$ (since \mathbf{W}_{II} has full column rank), where $\mathbf{B}_{II} \triangleq \mathbf{W}_{II} \mathbf{A}$. ■

5. NUMERICAL EXAMPLE

We illustrate the implication of Theorem 1 through a numerical example. Fig. 3 shows the singular values of \mathbf{B} for Arrays I and II given rank-2 waveform matrix \mathbf{S} in (6) with $s_{11} = s_{22} = s_{13} = 1/\sqrt{3}$ and $s_{12} = s_{21} = s_{23} = 0$. The smallest singular value of Array I is zero, whereas that of Array II is nonzero. Hence the Kruskal rank of Array I is

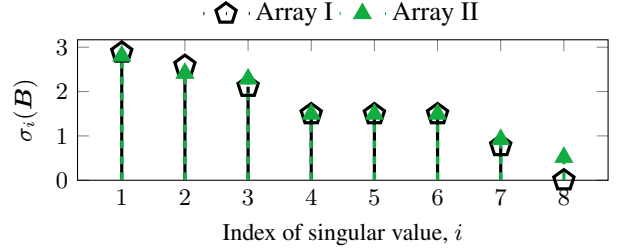


Fig. 3. Singular values of sensing matrix \mathbf{B} . This is rank-deficient in case of Array I—implying reduced Kruskal rank.

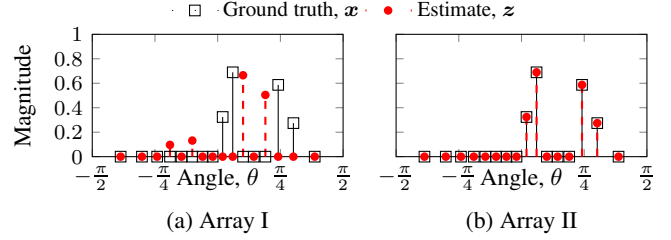


Fig. 4. Scatterer configuration that cannot be identified by Array I, but can be identified by Array II.

no larger than $N_\Sigma - 1 = 7$, since $\text{k-rank}(\mathbf{B}) \leq \text{rank}(\mathbf{B})$. Array I can thus unambiguously identify at most $\lfloor 7/2 \rfloor = 3$ scatterers. In contrast, Array II can identify 4 scatterers since its Kruskal rank is $N_\Sigma = 8$. This is demonstrated in Fig. 4, which shows a configuration of $K = 4$ scatterers (grid size $V = 16$) identifiable by Array II but not Array I. This example is representative of an autonomous sensing scenario where identifying weak scatterers (pedestrians) close to strong ones (vehicles) is critical. We identified the scatterers by solving the following optimization problem by exhaustive search: minimize $\|z\|_0$ subject to $\mathbf{y}_i = \mathbf{B}_i z$, where $i \in \{I, II\}$ refers to Arrays I and II, respectively. We note that infinitely many unidentifiable scatterer configurations, such as the one in Fig. 4, can be generated by straightforward linear algebraic manipulations when $\text{k-rank}(\mathbf{B}) < 2K$.

6. CONCLUSIONS

This paper investigated the role of the array redundancy pattern in active sensing. We showed that identifying the maximum number of scatterers requires carefully designing the redundancy pattern when employing fewer independent waveforms than transmitters. Specifically, an unfavorable choice of array geometry may fundamentally hamper identifiability such that no waveform will improve identifiability to the level of another array geometry employing the same (reduced) waveform rank, number of physical/virtual sensors, and identical (contiguous) sum co-array. Several open questions for future work emerge from this insight. For example, how severely can identifiability be affected by a poor choice of array or waveform? Furthermore, what impact does a reduced Kruskal rank have in practice when worst-case performance is not of primary interest?

7. REFERENCES

- [1] D. Ma, N. Shlezinger, T. Huang, Y. Liu, and Y. C. Eldar, “Joint radar-communication strategies for autonomous vehicles: Combining two key automotive technologies,” *IEEE Signal Processing Magazine*, vol. 37, no. 4, pp. 85–97, 2020.
- [2] S. Sun, A. P. Petropulu, and H. V. Poor, “MIMO radar for advanced driver-assistance systems and autonomous driving: Advantages and challenges,” *IEEE Signal Processing Magazine*, vol. 37, no. 4, pp. 98–117, 2020.
- [3] F. Liu, C. Masouros, A. P. Petropulu, H. Griffiths, and L. Hanzo, “Joint radar and communication design: Applications, state-of-the-art, and the road ahead,” *IEEE Transactions on Communications*, vol. 68, no. 6, pp. 3834–3862, 2020.
- [4] A. Hassanien, M. G. Amin, Y. D. Zhang, and F. Ahmad, “Signaling strategies for dual-function radar communications: an overview,” *IEEE Aerospace and Electronic Systems Magazine*, vol. 31, no. 10, pp. 36–45, 2016.
- [5] N. Levanon and E. Mozeson, *Radar Signals*. John Wiley & Sons, 2004.
- [6] P. Kumari, S. A. Vorobyov, and R. W. Heath, “Adaptive virtual waveform design for millimeter-wave joint communication–radar,” *IEEE Transactions on Signal Processing*, vol. 68, pp. 715–730, 2020.
- [7] P. Wang, P. Boufounos, H. Mansour, and P. V. Orlik, “Slow-time MIMO-FMCW automotive radar detection with imperfect waveform separation,” in *IEEE International Conference on Acoustics, Speech and Signal Processing (ICASSP)*, 2020, pp. 8634–8638.
- [8] M. Wang and A. Nehorai, “Coarrays, MUSIC, and the Cramér-Rao bound,” *IEEE Transactions on Signal Processing*, vol. 65, no. 4, pp. 933–946, Feb 2017.
- [9] E. Tohidi, M. Coutino, S. P. Chepuri, H. Behroozi, M. M. Nayebi, and G. Leus, “Sparse antenna and pulse placement for colocated MIMO radar,” *IEEE Transactions on Signal Processing*, vol. 67, no. 3, pp. 579–593, 2019.
- [10] S. Sedighi, B. S. Mysore R, M. Soltanalian, and B. Ottersten, “On the performance of one-bit DoA estimation via sparse linear arrays,” *IEEE Transactions on Signal Processing*, vol. 69, pp. 6165–6182, 2021.
- [11] P. Sarangi, M. C. Hücümenoğlu, and P. Pal, “Beyond coarray MUSIC: Harnessing the difference sets of nested arrays with limited snapshots,” *IEEE Signal Processing Letters*, vol. 28, pp. 2172–2176, 2021.
- [12] —, “Single-snapshot nested virtual array completion: Necessary and sufficient conditions,” *IEEE Signal Processing Letters*, vol. 29, pp. 2113–2117, 2022.
- [13] P. Sarangi, M. C. Hücümenoğlu, R. Rajamäki, and P. Pal, “Super-resolution with sparse arrays: A non-asymptotic analysis of spatio-temporal trade-offs,” *IEEE Transactions on Signal Processing*, pp. 1–14, 2023.
- [14] D. W. Bliss and K. W. Forsythe, “Multiple-input multiple-output (MIMO) radar and imaging: degrees of freedom and resolution,” in *37th Asilomar Conference on Signals, Systems and Computers*, vol. 1, 2003, pp. 54–59 Vol.1.
- [15] J. Li, P. Stoica, L. Xu, and W. Roberts, “On parameter identifiability of MIMO radar,” *IEEE Signal Processing Letters*, vol. 14, no. 12, pp. 968–971, 2007.
- [16] R. Rajamäki and P. Pal, “Array-informed waveform design for active sensing: Diversity, redundancy, and identifiability,” *arXiv*, 2023. [Online]. Available: <https://arxiv.org/abs/2305.06478v1>
- [17] C.-L. Liu and P. P. Vaidyanathan, “Robustness of difference coarrays of sparse arrays to sensor failures—Part I: A theory motivated by coarray MUSIC,” *IEEE Transactions on Signal Processing*, vol. 67, no. 12, pp. 3213–3226, 2019.
- [18] I. Bekkerman and J. Tabrikian, “Target detection and localization using MIMO radars and sonars,” *IEEE Transactions on Signal Processing*, vol. 54, no. 10, pp. 3873–3883, 2006.
- [19] B. Friedlander, “On signal models for MIMO radar,” *IEEE Transactions on Aerospace and Electronic Systems*, vol. 48, no. 4, pp. 3655–3660, 2012.
- [20] H. Jafarkhani, *Space-Time Coding: Theory and Practice*. Cambridge University Press, 2005.
- [21] R. T. Hoctor and S. A. Kassam, “The unifying role of the coarray in aperture synthesis for coherent and incoherent imaging,” *Proceedings of the IEEE*, vol. 78, no. 4, pp. 735–752, Apr 1990.
- [22] D. L. Donoho and M. Elad, “Optimally sparse representation in general (nonorthogonal) dictionaries via ℓ_1 minimization,” *Proceedings of the National Academy of Sciences*, vol. 100, no. 5, pp. 2197–2202, 2003.
- [23] P. Pal and P. P. Vaidyanathan, “Pushing the limits of sparse support recovery using correlation information,” *IEEE Transactions on Signal Processing*, vol. 63, no. 3, pp. 711–726, Feb 2015.